Accepted Manuscript

Potential forcings of summer temperature variability of the southeastern Tibetan Plateau in the past 12 ka

Enlou Zhang, Jie Chang, Weiwei Sun, Yanmin Cao, Peter Langdon, Jun Cheng

PII: S1367-9120(18)30103-2
DOI: https://doi.org/10.1016/j.jseaes.2018.03.023
Reference: JAES 3452

To appear in: *Journal of Asian Earth Sciences*

Received Date: 7 September 2017
Revised Date: 9 March 2018
Accepted Date: 20 March 2018

Please cite this article as: Zhang, E., Chang, J., Sun, W., Cao, Y., Langdon, P., Cheng, J., Potential forcings of summer temperature variability of the southeastern Tibetan Plateau in the past 12 ka, *Journal of Asian Earth Sciences* (2018), doi: https://doi.org/10.1016/j.jseaes.2018.03.023

Potential forcings of summer temperature variability of the southeastern Tibetan Plateau in the past 12 ka

Enlou Zhang[1*], Jie Chang[1,2], Weiwei Sun[1], Yanmin Cao[3], Peter Langdon[4], Jun Cheng[5]

1. State Key Laboratory of Lake Science and Environment, Nanjing Institute of Geography and Limnology, Chinese Academy of Sciences, Nanjing 210008, China
2. School of Earth and Environmental Sciences, The University of Queensland, St Lucia, Brisbane, Queensland, 4072, Australia
3. College of Resources and Environmental Science, South-Central University for Nationalities, Wuhan, 430074, China
4. Geography and Environment, University of Southampton, Southampton, SO171BJ, UK
5. Polar Climate System and Global Change Laboratory, Nanjing University of Information Science and Technology, Nanjing 210044, China

Abstract

Investigating potential forcing mechanisms of terrestrial summer temperature changes from the Asian summer monsoon influenced area is of importance to better understand the climate variability in these densely populated regions. The results of spectral and wavelet analyses of the published chironomid reconstructed mean July temperature data from Tiancai Lake on the SE Tibetan Plateau are presented. The evidence of solar forcing of the summer temperature variability from the site on centennial timescales where key solar periodicities (at 855±40, 465±40, 315±40 and 165±40 yr) are revealed. By using a band-pass filter, coherent fluctuations were found in the strength of Asian summer monsoon, Northern Hemisphere high latitude climate and high elevation mid-latitude (26 °N) terrestrial temperatures with solar sunspot cycles since about 7.6 ka. The two abrupt cooling events detected from the Tiancai Lake record, centered at ~9.7 and 3.5 ka were examined respectively. Coupled with the paleoclimate modelling results, the early Holocene event (9.7 ka) is possibly linked to an ocean-atmospheric feedback mechanism whereas the latter event (3.5 ka) may be more directly related to external forcing.

Key words: Asian summer monsoon, solar cycles, external forcing, terrestrial summer temperatures, southeast Tibetan Plateau

1. Introduction

The Asian summer monsoon (ASM), which includes the Indian Ocean and the East Asian summer monsoon subsystems, is a seasonal, tropical wind that brings moisture to the Asian continent during the boreal summer (An et al. 2001; Wu et al. 2012). It is a critical component of the global atmospheric system dominating the Asian climate, and is the primary water source for more than 50% of the world's population (Clift and Plumb 2008). Driven primarily by equator to pole thermal and atmospheric pressure gradients, the ASM has changed in intensity and strength over decadal to multi-millennial timescales (An et al. 2012a; An et al. 2001). Empirical and modeling studies have been used to attempt to detect past changes in the strength of the ASM (e.g. Cai et al. 2006; Cheng et al. 2016; Cook et al. 2011; Dykoski et al. 2005; Liu et al. 2012; Liu et al. 2009; Meng et al. 2017; Wang et al. 2001). Nonetheless, documenting past and future forcing mechanisms and variability of the ASM remains a challenge (Cheng et al. 2012; Clemens et al. 2010).

The Chinese stalagmite based $\delta^{18}O$ records (e.g. Dongge Cave and Sanbao Cave) (Dykoski et al. 2005; Wang et al. 2008) suggest that the ASM precipitation was primarily forced by insolation-induced variation at the orbital time scale (Cheng et al. 2012; Wang et al. 2008). In contrast, other studies suggest that a combined response to external forcing of the Northern Hemisphere, changes in ice volume, and latent heating of the southern Indian Ocean (Clemens et al. 2010) could be a better explanation for millennial changes in the ASM. Changes in solar activity have been widely proposed as a driving force of Holocene ASM variability on decadal to centennial scales (Bond et al. 2001; Fleitmann et al. 2003; Wang et al. 2005; Wanner et al. 2015). However, published proxy-based records invoking solar drivers of early to mid-Holocene ASM strength are not coherent (Mischke and Zhang 2010). These ambiguous records indicate a complex regional pattern of climate change related to the ASM during this period (An et al. 2000; Herzschuh 2006; Mischke et al. 2008). Tropical ocean surface temperature feedbacks and the seasonal variability of the monsoon are also potential factors influencing changes in precipitation over the Asian continent (Caley et al. 2014; Shi 2016; Shi et al. 2012). In summary, more studies are required to examine the impact of likely forcing mechanisms responsible for the monsoon variability throughout the entire Holocene across different timescales.

One way through which changes in ASM can be reconstructed is through analyses of proxy records from lake sediments. Chironomids are non-biting midges living in semi-permeant to permanent waterbodies. They have several attributes that make them useful as environmental indicators. Most notable is their temperature sensitivity, having a rapid response to summer temperature changes (Brooks et al. 2007). These characteristics enable us to produce multi-decadal resolution records over millennial timescales to test ideas of possible forcing mechanisms such as solar periodicities. Such records are relatively rare, as typically the response variable is not rapid enough to detect high resolution (multi-decadal) changes. For instance, vegetation (i.e. pollen records) usually has a delayed response to climate change of a few hundred years (Birks and Birks 2008), or often the records are not sampled at high resolution to perform these types of analyses (Wang et al. 2010).

Over millennial time scales, changes in the position of the intertropical convergence zone (ITCZ) significantly influences the strength of the ASM and the moisture regimes in the middle- to low-latitude Northern Hemisphere land regions (Fleitmann et al. 2007). Weakening of the Indian Summer Monsoon (ISM) decreases precipitation in the SE sector of the Tibetan Plateau while a stronger monsoonal flow increases precipitation. Currently, in Yunnan Province of the SE Tibetan Plateau, the highest average temperatures occur coincidently with the highest monthly precipitation, which is usually July (Zhang et al. 2017b). This relationship between moisture availability, mean July temperature and ASM strength implies that proxy-based reconstructions of mean July temperature and precipitation from the ASM affected areas could be used to infer the relative ASM strength, assuming this relationship also holds for the Holocene.

Using these relationships, published paleoclimate records were examined from a chironomid-based terrestrial mean July temperature record from Tiancai Lake, SE Tibetan Plateau (Zhang et al. 2017a). The record was compared with a solar irradiance reconstruction, $\delta^{18}O$ stalagmites recorded the strength of the ASM from Dongge Cave, and North Atlantic climate as reconstructed through the Greenland ice core record (Fig. 1) to identify whether the mid-latitude high elevation site (Tiancai Lake, 26 °N, 3898 m a.s.l) showed coherent changes with the strength of the ASM. Whether these changes are linked to the Northern Hemisphere high latitudes and solar irradiance in the Holocene were further tested. The chironomid record from Tiancai Lake was validated in Zhang et al. (2017a,b) as a reliable summer temperature reconstruction.

This record allowed us to separate a seasonal temperature signal from precipitation effects which were difficult to achieve from previous studies (Xiao et al. 2014). These analyses were coupled with the comparison to TraCE-21000 simulated results (Liu et al. 2009) to decipher past changes in the ASM influence and the possible forcings over different timescales during the Holocene.

2. Materials and methods

The SE margin of the Tibetan Plateau is characterized by warm-humid summers and cold-dry winters, influenced by the interaction of the Indian Ocean summer monsoon and the southern branch of the Northern Hemisphere westerly in winter (Fig. 1). Most of the annual precipitation occurs during May and September in this region, which is the wet season due to the monsoon activity (Böhner 1994). Tiancai Lake has a mean July temperature of 8.4 °C and a mean annual temperature of 2.5 °C at present day. Tiancai Lake (26°38′3.8″N, 99°43′00″E, 3898 m a.s.l.) (Fig. 1) is glacially formed and located on the Hengduan mountain range in the SE margin of the Tibetan Plateau. The mean water depth is 6 m and is located about 200 m below the tree-line at present. The main composition of catchment vegetation includes *Abies* and *Picea* forest, and Rhododendron shrubs (Xiao et al. 2014). There is very limited human disturbance around the lake. More details of Tiancai Lake are also available in Xiao et al. (2014), Chen et al. (2014) and Zhang et al. (2017a,b).

This study is based on the data from the high resolution (~50 year average) chironomid record published in Zhang et al. (2017a). The record was based on a 927-cm long sediment core (TCK1) recovered in 2008 from the centre of Tiancai

Lake. Chironomid samples were taken from the same core (TCK1) as the pollen record described in Xiao et al. (2014). The chronological model for TCK1 was based on fifteen terrestrial macrofossil plant samples and the final age-depth model is presented and described in Zhang et al. (2017a), Xiao et al. (2014) and Chen et al. (2014), respectively. The average radiocarbon dating error is ± 40 years over the last 12 ka (Xiao et al., 2014). The Holocene (the last ~12 ka) mean July air temperatures of Tiancai Lake were quantified applying the chironomid-based transfer function developed using 100 lakes from SW China (Zhang et al. 2017b). The reconstructed temperature values and trends were examined using several reconstruction diagnostic methods and the results suggest that the reconstructed mean July temperature data is reliable (Zhang et al. 2017a; Zhang et al. 2017b).

In this study, spectral and wavelet analysis were performed to investigate the periodicities preserved in the Tiancai Lake temperature record. Spectral analysis was conducted using REDFIT 3.8 described from Schulz and Mudelsee (2002): The spectra were first estimated using the Lomb-Scargle Fourier Transform for unevenly spaced data and the analysis showed that the oversampling factor (OFAC) and maximum frequency (HIFAC) are 2 and 1 respectively; the Welch-Overlapped-Segment-Averaging procedure with 50% overlapped segments was then applied for univariate spectra. A Welch window type was used to reduce spectral leakage and the univariate spectra were then bias-corrected using 1000 Monte-Carlo simulation. Based on the chi-square test, the significant periodicities above the 90 and 95% confidence level were selected.

For wavelet analysis, the reconstructed mean July temperatures were first interpolated to evenly spaced data and a wavelet power spectrum was then applied (Torrence and Compo 1998); the wavelet coefficients were calculated by the Morlet continuous wavelet transform (CWT); red and blue colours were used to indicate high and low powers (from 64 to 1/64) respectively; areas which represent significant cycles with the confidence level greater than 95% were circled by black solid lines. A Gaussian band-pass filter (400-600 year band-pass) (Holloway 1958) was then employed to reveal the signature of the dominant cycles and coherence within four proxy-based data sets (the chironomid-based temperature, total solar irradiance reconstruction, $\delta^{18}O$ of GISP2 and Dongge Cave stalagmite $\delta^{18}O$ data sets respectively).

Finally, the proxy record was compared with the temperature outputs from the TraCE-21000 model (Liu et al. 2009). It is a transient simulation of the global climate of the last 21 ka in the community climate system model version 3 (CCSM3) of the National Center for Atmospheric Research (NCAR) (Collins et al. 2006). The simulation is forced by realistic climatic forcing factors, including orbital insolation (Berger 1978), atmospheric greenhouse gases concentration (GHGs) (Joos and Spahni 2008), melt water discharge (McManus et al. 2004), the continental ice sheets derived from ICE-5G (Peltier 2004) and the modification of coastlines and bathymetry at 13.1, 12.9, 7.6 and 6.2 ka for the Barents Sea, the Bering Strait, Hudson Bay and the Indonesian through flow, respectively (He 2011).

3. Results

The Tiancai Lake chironomid record shows a similar general trend at the millennial scale with several high resolution palaeoclimate records from the ASM regions such as stalagmite $\delta^{18}O$ records from Dongge cave, SE China and Qunf cave, south Oman (Fleitmann et al. 2007; Wang et al. 2005; Zhang et al. 2017a). This record demonstrates high frequency variations at centennial to millennial scales. The spectral analysis reveals a number of centennial cycles during the Holocene. The results show statistically significant (spectral peaks above 90% confidence level) centennial periodicities centered at 855±40, 465±40, 315±40, 165±40 yr and 117±40 (Fig. 2A). The original resolution of the chironomid inferred temperature data that we performed spectral analyses on is ~50 years on average, and hence the detected periods at 117±40 and 165±40 yr should be treated with caution. The result of the wavelet analysis shows that ~500-year quasi-periodic oscillations of Tiancai Lake summer temperatures are the most stable and dominant among these periodicities during the last 12 ka (Fig. 2B).

These results are similar to cycles of total solar irradiance (TSI) reconstructed from cosmic radiation ^{10}Be and $\Delta^{14}C$ (Eddy cycle around 1000, 500, 350 and 148 yr) within age uncertainties (Soon et al. 2014; Steinhilber et al. 2012; Wanner et al. 2008). These periodicities are also reported by other records from the ASM regions and around the North Atlantic, including the stalagmite $\delta^{18}O$ record of Dongge Cave (south China) that revealed the 957, 558 and 159-yr periodicities (Wang et al. 2005); lacustrine calcite stable isotope records from the NE United States which showed the 500 and 330-yr periodicities (Zhao et al. 2010); variations in sediment lightness from the North Atlantic that are characterized by cyclicities equivalent to 1000 and 550 yr (Chapman and Shackleton 2000); surface wetness cycles of 1100 years from a peat bog in Scotland (Langdon et al. 2003); biogenic silica content in Arolik Lake from the Alaskan subarctic which showed the 950, 435 and 170 yr periodicities (Hu et al. 2003); and pollen-based reconstruction from Lake Xiaolongwan, which suggests a dominant 500-year climate cycle from the East Asian summer monsoon region (Xu et al. 2014). More recently, marine sediment records from Indian Ocean (Oman margin) (Munz et al. 2017) and lake records from southern India (Warrier et al. 2017) also show these solar cycles. The implication is that this regional variability could possibly represent a regional to global pattern as a response to external forcing.

Band-pass filter outputs (after the 400-600 year band pass filter) of our chironomid-based temperature reconstructions comparing the TSI (Steinhilber et al. 2012), $\delta^{18}O$ of GISP2 (Grootes et al. 1993) and Dongge Cave stalagmite $\delta^{18}O$ records (Wang et al. 2005) are shown in Figure 3. The cave deposits inferred monsoon intensity data were used together here because on the orbital to suborbital timescale, an overall positive relationship between temperature and Asian monsoon precipitation was demonstrated (Marcott et al. 2013). Amplitude modulations of the filter outputs of both the TSI and our record for the past 9.4 ka run largely synchronous, in particular from ~7.6 ka to the present (Fig. 3A). General co-variability of the band-pass filtered chironomid-inferred summer temperature time series with the $\delta^{18}O$ record of GISP2 for was also observed (Fig. 3B). The Tiancai Lake record and Dongge Cave $\delta^{18}O$ stalagmite data sets are both in-phase except for a disconnection between ~8.4-6.4 ka. The phase variation during the early Holocene is not unexpected because the forcing-response mechanism is complex. One of the many reasons that could lead to the disparity was the dating uncertainties in the proxy-based records. In addition, proxies also represent different seasons. For instance, GISP2 may characterize a winter forcing factor while a chironomid temperature record is likely showing a non-linear summer response (Clegg et al. 2011).

In summary, regardless of the exact correlation of signals, the amplitude modulation of Tiancai Lake record in the 400-600 year bandwidth are in-phase with amplitude modulation of solar irradiance, Greenland ice core and ASM records since 7.6 ka. The chironomid-based record from Tiancai Lake therefore provides further evidence that solar forcing was persistently modulating summer temperature variability of the SE Tibetan Plateau. This was possibly achieved by changing the strength of the Indian Ocean summer monsoon since ~7.6 ka (approximately ~3 ka after the summer insolation maximum) through thermohaline circulations or complex atmospheric feedbacks. The results are supported by various Indian Ocean monsoon records, in particular from the high resolution Qunf Cave speleothems $\delta^{18}O$ record, *G. bulloides* and sea surface temperature and upwelling records from NW Arabian Sea (Fleitmann et al. 2003; Gupta et al. 2005; Munz et al. 2017).

4. Discussion

Changes of solar irradiance can directly influence the continent surface temperature variation and ocean-atmospheric circulations (Gray et al. 2010; Shindell et al. 2001; Wang and Dickinson 2013). When TSI is reduced, the downward-propagating effects were triggered by changes in the top of the atmosphere. This leads to a cooling of the stratosphere and the Northern Hemisphere generally experiences cooler climates (Kaufmann et al. 2011; Shindell et al. 1999; Wang and Dickinson 2013). In addition, sensitive atmospheric responses around the North Atlantic region to reduced TSI could reduce North Atlantic Deep Water (NADW) intensity, cool the ocean surface temperature and trigger the southward migration of the mid-latitude westerlies and the mean position of the ITCZ (Shindell et al. 2001). Thus during periods of cool summers, the weak summer monsoon circulation was caused by a decreased land-ocean thermal difference and southerly shift in ITCZ. This effect could reduce the latent heat released by monsoon precipitation over the Asian continent, which intensifies the cooling in summer (An et al. 2012b; Duan and Wu 2005; Wang et al. 2005). In summary, our findings indicate that centennial solar variability associated with NADW anomalies could regulate summer temperature variations over the SE Tibetan Plateau throughout at least the past 7.6 ka.

Paleoclimate models have been developed over the last decade to explore the regional temperature responses to various forcings in the Holocene (Braconnot et al. 2012; Braconnot et al. 2007; Jiang et al. 2013; Jiang et al. 2015). The TraCE-21000 simulated temperature data covering the period of 12 ka to ca. 0 ka (Liu et al. 2009) were selected. It has been demonstrated that this simulation could model deglacial and Holocene climate changes that were consistent with a number of proxy records at global and regional scales (Otto-Bliesner et al. 2014; Shakun et al. 2012). Furthermore, TraCE-21000 showed an ability to provide reasonable simulations for the long-term change of the Asian monsoons since the last glacial maximum (Wen et al. 2016). The model was run to produce a temporal resolution of 100 years, making the output data comparable with the Tiancai Lake chironomid record. The results show that the simulated temperature response generally matches well with the long-term trend of the chironomid-based summer temperature reconstructions throughout the Holocene (Fig 4A and B). It was suggested that the overall pattern in summer temperatures of this region is likely responding to complex feedbacks in high altitude climate change on the millennial to multi-millennial scale, superimposed by multi-decadal to centennial timescale changes in TSI.

In the early Holocene, the summer temperature reconstructed from Tiancai Lake is characterized by a few apparent millennial-scale cool events despite the summer insolation reaching its maximum. The most pronounced early Holocene cool summer events in Tiancai occurred at between ~10.5 and 9.5 ka, centred at around 9.7 ka (Fig 4A). The summer temperature reached a minimum of ~7 °C (1.4 °C lower than the present day). This cooling period is recorded by several previous paleoclimate reconstructions from the adjacent region within the uncertainties of age model. Lower organic matter and reduced total pollen concentrations from Shudu Lake in northwest Yunnan Province suggest a cold period at about 10 ka (Cook et al. 2013). Records from Lake Ximencuo and Hongyuan peat in the NE QTP showed a significant cold spell centered at 10.2 ka (Cook et al. 2013; Mischke and Zhang 2010). This is also confirmed by the multi-proxy based climate record from Qinghai Lake, NE QTP (Shen et al. 2005), Guliya ice core (Thompson et al. 1997) from the northern QTP and the Muztag Ata and Kongur Shan glacier records (Seong et al. 2009) from the western margin of the QTP.

Wanner et al. (2014) argue that the early Holocene cold events were largely due to the relative collapse of Atlantic Meridional Overturning Circulation (AMOC), but this may be reduced in impact in the tropics and this far East, away from the North Atlantic. In an effort to elucidate the possible forcings of this millennial abrupt change in the early Holocene for this region, each component in the output of the transient model simulation results (Fig 4B-F) were further examined. This millennial cooling period could be driven by a complex internal feedback mechanism rather than external forcing because insolation is at maximum. The cooling is possibly linked to the forcing of meltwater influx in North Atlantic and Gulf Mexico (Fig. 4C) (Liu et al. 2009). This is also related to snow cover change in Eurasia and phase shift of the North Atlantic Oscillation (NAO). The change in snow accumulation in high latitudes and +/- NAO could drive the temperature changes in the mid-latitudes of the Asian continent through changing the atmospheric and oceanic teleconnections (Barnett et al. 1989).

In the later Holocene, the Tiancai Lake record displays an abrupt cooling of 1.6 °C (at ~6.8 °C) compared to the present day centred at around 3.5 ka. This is also recorded from a pollen-based study from an Alpine peat in northern India, which inferred a sharp decrease in Indian summer monsoon strength from 4-3.5 ka (Phadtare 2000). These findings are supported by environmental archeology evidence from both northern and southern China that suggested a large cultural collapse after 4 ka, as responses to climate deterioration (as reviewed in Liu and Feng (2012)). This abrupt cooling event is likely amplified by the continuous reduction of summer insolation, as shown in the simulated temperature response in the TraCE21000 (Fig. 4F). In addition, a synthesized data review of Holocene climate variability and forcing mechanisms (Wanner et al. 2015; Wanner et al. 2011) concludes that the later Holocene cold events (for instance after 4 ka), were likely influenced by co-varying drivers, notably the major tropical volcanic events and changes in Grand Solar Minima. The summer temperature reconstructions from the SE Tibetan Plateau provide evidence which supports these proposed mechanisms in general.

5. Conclusions

The 12 ka long and high resolution (average ~50-year) chironomid-based summer temperature record from the SE Tibetan Plateau provides a unique opportunity to examine the drivers of the climate variability in the region from a multi-decadal to multi-millennial timescale. Based on the summer temperatures from the SE Tibetan Plateau and collation of paleoclimate data, the study provides lines of evidence corroborating previous studies that the ASM strength, Northern Hemisphere high latitudes and high elevation mid-latitudes (26 °N) temperatures fluctuate in coherence to solar sunspot cycles since about 7.6 ka. The analyses revealed significant (at 90% confidence interval) periodicities centred at 855±40, 465±40, 315±40 and 165±40 year from Tiancai Lake whereas the ~500 year periodicity is likely the most dominant and stable. Our results suggest that on the multi-decadal to centennial timescale, the SE Tibetan Plateau summer climate was determined by solar-forced high-northern-latitude temperature variations, which drove meridional migration of the ITCZ over this period of the Holocene. However, different mechanisms likely pervade in the early and later Holocene abrupt cool events (e.g. cooling periods centered at 9.7 ka and 3.5 ka respectively). The study suggests that temperature instability was possibly caused by an ocean-atmospheric feedback mechanism during the first 3 ka of the Holocene whereas external forcing could have played a more significant role for the later Holocene event.

Acknowledgement: We thank X.Y. Xiao, Y.L. Li, X Chen, E.F. Liu, J.J. Wang, and Y. Wang (NIGLAS, Chinese Academy of Sciences) for field assistance. We also thank D.L. Ning and J.L. Wang for their help on the graphic preparation. This research is supported by the Program of Global Change and Mitigation (2016YFA0600502), the National Natural Science Foundation of China (No. 41572337).

References

An, Z., S. M. Colman, W. Zhou, X. Li, E. T. Brown, A. J. T. Jull, Y. Cai, Y. Huang, X. Lu, H. Chang, Y. Song, Y. Sun, H. Xu, W. Liu, Z. Jin, X. Liu, P. Cheng, Y. Liu, L. Ai, X. Li, X. Liu, L. Yan, Z. Shi, X. Wang, F. Wu, X. Qiang, J. Dong, F. Lu & X. Xu, 2012a. Interplay between the Westerlies and Asian monsoon recorded in Lake Qinghai sediments since 32 ka. Scientific Reports 2, 619

An, Z., S. M. Colman, W. Zhou, X. Li, E. T. Brown, A. J. T. Jull, Y. Cai, Y. Huang, X. Lu, H. Chang, Y. Song, Y. Sun, H. Xu, W. Liu, Z. Jin, X. Liu, P. Cheng, Y. Liu, L. Ai, X. Li, X. Liu, L. Yan, Z. Shi, X. Wang, F. Wu, X. Qiang, J. Dong, F. Lu & X. Xu, 2012b. Interplay between the Westerlies and Asian monsoon recorded in Lake Qinghai sediments since 32 ka. Scientific Reports 2

An, Z., J. E. Kutzbach, W. L. Prell & S. C. Porter, 2001. Evolution of Asian monsoons and phased uplift of the Himalaya-Tibetan plateau since Late Miocene times. Nature 411, 62-66.

An, Z., S. C. Porter, J. E. Kutzbach, W. Xihao, W. Suming, L. Xiaodong, L. Xiaoqiang & Z. Weijian, 2000. Asynchronous Holocene optimum of the East Asian monsoon. Quaternary Science Reviews 19, 743-762

Barnett, T. P., L. Dümenil, U. Schlese, E. Roeckner & M. Latif, 1989. The Effect of Eurasian Snow Cover on Regional and Global Climate Variations. Journal of the Atmospheric Sciences 46, 661-686.

Berger, A., 1978. Long-Term Variations of Daily Insolation and Quaternary Climatic Changes. Journal of the Atmospheric Sciences 35, 2362-2367

Birks, H. J. B. & H. H. Birks, 2008. Biological responses to rapid climate change at the Younger Dryas—Holocene transition at Kråkenes, western Norway. The Holocene 18, 19-30

Böhner, J., 1994. Circulation and representativeness of precipitation and air temperature in the southeast of the Qinghai-Xizang Plateau. GeoJournal 34, 55-66

Bond, G., B. Kromer, J. Beer, R. Muscheler, M. N. Evans, W. Showers, S. Hoffmann, R. Lotti-Bond, I. Hajdas & G. Bonani, 2001. Persistent Solar Influence on North Atlantic Climate During the Holocene. Science 294, 2130-2136

Braconnot, P., S. P. Harrison, M. Kageyama, P. J. Bartlein, V. Massondelmotte, A. Abeouchi, B. Ottobliesner & Y. Zhao, 2012. Evaluation of climate models using palaeoclimatic data. Nature Climate Change 2, 417-424.

Braconnot, P., B. Otto-Bliesner, S. Harrison, S. Joussaume, J. Y. Peterchmitt, A. Abe-Ouchi, M. Crucifix, E. Driesschaert, T. Fichefet, C. D. Hewitt, M. Kageyama, A. Kitoh, A. Laîné, M. F. Loutre, O. Marti, U. Merkel, G. Ramstein, P. Valdes, S. L. Weber, Y. Yu & Y. Zhao, 2007. Results of PMIP2 coupled simulations of the Mid-Holocene and Last Glacial Maximum Part 1: experiments and large-scale features. Clim Past 3, 261-277

Brooks, S. J., P. G. Langdon & O. Heiri, 2007. The Identification and Use of Palaearctic Chironomidae Larvae in Palaeoecology. Quaternary Research Association, London, UK.

Cai, Y., Z. An, H. Cheng, R. L. Edwards, M. J. Kelly, W. Liu, X. Wang & C.-C. Shen, 2006. High-resolution absolute-dated Indian Monsoon record between 53 and 36 ka from Xiaobailong Cave, southwestern China. Geology 34, 621-624

Caley, T., D. M. Roche & H. Renssen, 2014. Orbital Asian summer monsoon dynamics revealed using an isotope-enabled global climate model. Nature Communications 5, 5371.

Chapman, M. R. & N. J. Shackleton, 2000. Evidence of 550-year and 1000-year cyclicities in North Atlantic circulation patterns during the Holocene. The Holocene 10, 287-291

Chen, X., Y. Li, S. Metcalfe, X. Xiao, X. Yang & E. Zhang, 2014. Diatom response to Asian monsoon variability during the Late Glacial to Holocene in a small treeline lake, SW China. The Holocene 24, 1369-1377

Cheng, H., R. L. Edwards, A. Sinha, C. Spötl, L. Yi, S. Chen, M. Kelly, G. Kathayat, X. Wang, X. Li, X. Kong, Y. Wang, Y. Ning & H. Zhang, 2016. The Asian monsoon over the past 640,000 years and ice age terminations. Nature 534, 640-646

Cheng, H., A. Sinha, X. Wang, F. W. Cruz & R. L. Edwards, 2012. The Global Paleomonsoon as seen through speleothem records from Asia and the Americas. Climate Dynamics 39, 1045-1062

Clegg, B. F., R. Kelly, G. H. Clarke, I. R. Walker & F. S. Hu, 2011. Nonlinear response of summer temperature to Holocene insolation forcing in Alaska. Proceedings of the National Academy of Sciences 108, 19299-19304

Clemens, S. C., W. L. Prell & Y. Sun, 2010. Orbital-scale timing and mechanisms driving Late Pleistocene Indo-Asian summer monsoons: Reinterpreting cave speleothem δ18O. Paleoceanography 25, n/a-n/a

Clift, P. D. & R. A. Plumb, 2008. The Asian monsoon: causes, history and effects. Cambridge University Press, Cambridge, UK.

Collins, W. D., C. M. Bitz, M. L. Blackmon, G. B. Bonan, C. S. Bretherton, J. A. Carton, P. Chang, S. C.

Doney, J. J. Hack, T. B. Henderson, J. T. Kiehl, W. G. Large, D. S. McKenna, B. D. Santer & R. D. Smith, 2006. The Community Climate System Model Version 3 (CCSM3). Journal of Climate 19, 2122-2143

Cook, C. G., R. T. Jones, P. G. Langdon, M. J. Leng & E. Zhang, 2011. New insights on Late Quaternary Asian palaeomonsoon variability and the timing of the Last Glacial Maximum in southwestern China. Quaternary Science Reviews 30, 808-820

Cook, C. G., R. T. Jones & C. S. M. Turney, 2013. Catchment instability and Asian summer monsoon variability during the early Holocene in southwestern China. Boreas 42, 224-235

Duan, A. M. & G. X. Wu, 2005. Role of the Tibetan Plateau thermal forcing in the summer climate patterns over subtropical Asia. Climate Dynamics 24, 793-807

Dykoski, C. A., R. L. Edwards, H. Cheng, D. Yuan, Y. Cai, M. Zhang, Y. Lin, J. Qing, Z. An & J. Revenaugh, 2005. A high-resolution, absolute-dated Holocene and deglacial Asian monsoon record from Dongge Cave, China. Earth and Planetary Science Letters 233, 71-86

Fleitmann, D., S. J. Burns, A. Mangini, M. Mudelsee, J. Kramers, I. Villa, U. Neff, A. A. Al-Subbary, A. Buettner, D. Hippler & A. Matter, 2007. Holocene ITCZ and Indian monsoon dynamics recorded in stalagmites from Oman and Yemen (Socotra). Quaternary Science Reviews 26, 170-188

Fleitmann, D., S. J. Burns, M. Mudelsee, U. Neff, J. Kramers, A. Mangini & A. Matter, 2003. Holocene Forcing of the Indian Monsoon Recorded in a Stalagmite from Southern Oman. Science 300, 1737-1739

Gray, L. J., J. Beer, M. Geller, J. D. Haigh, M. Lockwood, K. Matthes, U. Cubasch, D. Fleitmann, G. Harrison, L. Hood, J. Luterbacher, G. A. Meehl, D. Shindell, B. van Geel & W. White, 2010. Solar influences on climate. Reviews of Geophysics 48, RG4001

Grootes, P. M., M. Stuiver, J. W. C. White, S. Johnsen & J. Jouzel, 1993. Comparison of oxygen isotope records from the GISP2 and GRIP Greenland ice cores. Nature 366, 552-554.

Gupta, A. K., M. Das & D. M. Anderson, 2005. Solar influence on the Indian summer monsoon during the Holocene. Geophysical Research Letters 32, n/a-n/a

He, F., 2011. Simulating Transient Climate Evolution of the Last Deglaciation with CCSM3 Univ. Wisconsin-Madison.

Herzschuh, U., 2006. Palaeo-moisture evolution in monsoonal Central Asia during the last 50,000 years. Quaternary Science Reviews 25, 163-178

Holloway, J. L., 1958. Smoothing and Filtering of Time Series and Space Fields. Advances in Geophysics 4, 351-389

Hu, F. S., D. Kaufman, S. Yoneji, D. Nelson, A. Shemesh, Y. Huang, J. Tian, G. Bond, B. Clegg & T. Brown, 2003. Cyclic variation and solar forcing of Holocene climate in the Alaskan subarctic. Science 301, 1890.

Jiang, D., X. Lang, Z. Tian & L. Ju, 2013. Mid-Holocene East Asian summer monsoon strengthening: Insights from Paleoclimate Modeling Intercomparison Project (PMIP) simulations. Palaeogeography Palaeoclimatology Palaeoecology 369, 422-429.

Jiang, D., Z. Tian & X. Lang, 2015. Mid-Holocene global monsoon area and precipitation from PMIP simulations. Climate Dynamics 44, 2493-2512

Joos, F. & R. Spahni, 2008. Rates of change in natural and anthropogenic radiative forcing over the past 20,000 years. Proceedings of the National Academy of Sciences 105, 1425-1430

Kaufmann, R. K., H. Kauppi, M. L. Mann & J. H. Stock, 2011. Reconciling anthropogenic climate change with observed temperature 1998-2008. Proceedings of the National Academy of Sciences of the United States of America 108, 11790-11793

Langdon, P. G., K. E. Barber & P. D. M. Hughes, 2003. A 7500-year peat-based palaeoclimatic reconstruction and evidence for an 1100-year cyclicity in bog surface wetness from Temple Hill Moss, Pentland Hills, southeast Scotland. Quaternary Science Reviews 22, 259-274

Liu, F. & Z. Feng, 2012. A dramatic climatic transition at ~4000 cal. yr BP and its cultural responses in Chinese cultural domains. The Holocene 22, 1181-1197

Liu, Z., A. E. Carlson, F. He, E. C. Brady, B. L. Otto-Bliesner, B. P. Briegleb, M. Wehrenberg, P. U. Clark, S. Wu, J. Cheng, J. Zhang, D. Noone & J. Zhu, 2012. Younger Dryas cooling and the Greenland climate response to CO2. Proceedings of the National Academy of Sciences 109, 11101-11104

Liu, Z., B. L. Otto-Bliesner, F. He, E. C. Brady, R. Tomas, P. U. Clark, A. E. Carlson, J. Lynch-Stieglitz, W. Curry, E. Brook, D. Erickson, R. Jacob, J. Kutzbach & J. Cheng, 2009. Transient Simulation of Last Deglaciation with a New Mechanism for Bølling-Allerød Warming. Science 325, 310-314

Marcott, S. A., J. D. Shakun, P. U. Clark & A. C. Mix, 2013. A Reconstruction of Regional and Global Temperature for the Past 11,300 Years. Science 339, 1198-1201

McManus, J. F., R. Francois, J. M. Gherardi, L. D. Keigwin & S. Brown-Leger, 2004. Collapse and rapid resumption of Atlantic meridional circulation linked to deglacial climate changes. Nature 428, 834

Meng, Y., W. Wang, J. Hu, J. Zhang & Y. Lai, 2017. Vegetation and climate changes over the last 30 000 years on the Leizhou Peninsula, southern China, inferred from the pollen record of Huguangyan Maar Lake. Boreas, n/a-n/a

Mischke, S., M. Kramer, C. Zhang, H. Shang, U. Herzschuh & J. Erzinger, 2008. Reduced early Holocene moisture availability in the Bayan Har Mountains, northeastern Tibetan Plateau, inferred from a multi-proxy lake record. Palaeogeography Palaeoclimatology Palaeoecology 267, 59-76

Mischke, S. & C. Zhang, 2010. Holocene cold events on the Tibetan Plateau. Global and Planetary Change 72, 155-163

Munz, P. M., S. Steinke, A. Böll, A. Lückge, J. Groeneveld, M. Kucera & H. Schulz, 2017. Decadal resolution record of Oman upwelling indicates solar forcing of the Indian summer monsoon (9–6 ka). Clim Past 13, 491-509

Otto-Bliesner, B. L., J. M. Russell, P. U. Clark, Z. Liu, J. T. Overpeck, B. Konecky, P. deMenocal, S. E. Nicholson, F. He & Z. Lu, 2014. Coherent changes of southeastern equatorial and northern African rainfall during the last deglaciation. Science 346, 1223-1227

Peltier, W. R., 2004. Global glacial isostasy and the surface of the ice-age earth: The ICE-5G (VM2) Model and GRACE. Annual Review of Earth and Planetary Sciences 32, 111-149

Phadtare, N. R., 2000. Sharp Decrease in Summer Monsoon Strength 4000–3500 cal yr B.P. in the Central Higher Himalaya of India Based on Pollen Evidence from Alpine Peat. Quaternary Research 53, 122-129

Schulz, M. & M. Mudelsee, 2002. REDFIT: estimating red-noise spectra directly from unevenly spaced paleoclimatic time series. Computers & Geosciences 28, 421-426

Seong, Y. B., L. A. Owen, C. Yi & R. C. Finkel, 2009. Quaternary glaciation of Muztag Ata and Kongur Shan: Evidence for glacier response to rapid climate changes throughout the Late Glacial and Holocene in westernmost Tibet. Geological Society of America Bulletin 121, 348-365

Shakun, J. D., P. U. Clark, F. He, S. A. Marcott, A. C. Mix, Z. Liu, B. Otto-Bliesner, A. Schmittner & E. Bard, 2012. Global warming preceded by increasing carbon dioxide concentrations during the last deglaciation. Nature 484, 49-54

Shen, J., X. Liu, M. Ryo, S. Wang & X. Yang, 2005. A high-resolution climatic change since the Late Glacial Age inferred from multi-proxy of sediments in Qinghai Lake. Science in China Series D: Earth Sciences 48, 742-751

Shi, Z., 2016. Response of Asian summer monsoon duration to orbital forcing under glacial and interglacial conditions: Implication for precipitation variability in geological records. Quaternary Science Reviews 139, 30-42.

Shi, Z., X. Liu & X. Cheng, 2012. Anti-phased response of northern and southern East Asian summer precipitation to ENSO modulation of orbital forcing. Quaternary Science Reviews 40, 30-38.

Shindell, D., D. Rind, N. Balachandran, J. Lean & P. Lonergan, 1999. Solar cycle variability, ozone, and climate. Science 284, 305.

Shindell, D. T., G. A. Schmidt, M. E. Mann, D. Rind & A. Waple, 2001. Solar forcing of regional climate change during the Maunder Minimum. Science 294, 2149-2152.

Soon, W., V. M. Velasco Herrera, K. Selvaraj, R. Traversi, I. Usoskin, C.-T. A. Chen, J.-Y. Lou, S.-J. Kao, R. M. Carter, V. Pipin, M. Severi & S. Becagli, 2014. A review of Holocene solar-linked climatic variation on centennial to millennial timescales: Physical processes, interpretative frameworks and a new multiple cross-wavelet transform algorithm. Earth-Science Reviews 134, 1-15

Steinhilber, F., J. A. Abreu, J. Beer, I. Brunner, M. Christl, H. Fischer, U. Heikkilä, P. W. Kubik, M. Mann & K. G. McCracken, 2012. 9,400 years of cosmic radiation and solar activity from ice cores and tree rings. Proceedings of the National Academy of Sciences of the United States of America 109, 5967-5971.

Thompson, L. G., T. Yao, M. E. Davis, K. A. Henderson, E. Mosley-Thompson, P.-N. Lin, J. Beer, H.-A. Synal, J. Cole-Dai & J. F. Bolzan, 1997. Tropical Climate Instability: The Last Glacial Cycle from a Qinghai-Tibetan Ice Core. Science 276, 1821-1825

Torrence, C. & G. P. Compo, 1998. A Practical Guide to Wavelet Analysis. Bulletin of the American Meteorological Society 79, 61-78

Wang, K. C. & R. E. Dickinson, 2013. Contribution of solar radiation to decadal temperature variability over land. Proceedings of the National Academy of Sciences of the United States of America 110, 14877-14882

Wang, Y., H. Cheng, R. L. Edwards, Y. He, X. Kong, Z. An, J. Wu, M. J. Kelly, C. A. Dykoski & X. Li, 2005. The Holocene Asian Monsoon: Links to Solar Changes and North Atlantic Climate. Science 308, 854-857

Wang, Y. B., X. Liu & U. Herzschuh, 2010. Asynchronous evolution of the Indian and East Asian Summer Monsoon indicated by Holocene moisture patterns in monsoonal central Asia. Earth-Science Reviews 103, 135-153

Wang, Y. J., H. Cheng, R. L. Edwards, Z. S. An, J. Y. Wu, C.-C. Shen & J. A. Dorale, 2001. A High-Resolution Absolute-Dated Late Pleistocene Monsoon Record from Hulu Cave, China. Science 294, 2345-2348

Wang, Y. J., H. Cheng, R. L. Edwards, X. Kong, X. Shao, S. Chen, J. Wu, X. Jiang, X. Wang & Z. An, 2008. Millennial- and orbital-scale changes in the East Asian monsoon over the past 224,000[thinsp]years. Nature 451, 1090-1093

Wanner, H., J. Beer, J. Bütikofer, T. J. Crowley, U. Cubasch, J. Flückiger, H. Goosse, M. Grosjean, F. Joos, J. O. Kaplan, M. Küttel, S. A. Müller, I. C. Prentice, O. Solomina, T. F. Stocker, P. Tarasov, M.

Wagner & M. Widmann, 2008. Mid- to Late Holocene climate change: an overview. Quaternary Science Reviews 27, 1791-1828

Wanner, H., L. Mercolli, M. Grosjean & S. P. Ritz, 2015. Holocene climate variability and change; a data-based review. Journal of the Geological Society 172, 254-263

Wanner, H., O. Solomina, M. Grosjean, S. P. Ritz & M. Jetel, 2011. Structure and origin of Holocene cold events. Quaternary Science Reviews 30, 3109-3123

Warrier, A. K., K. Sandeep & R. Shankar, 2017. Climatic periodicities recorded in lake sediment magnetic susceptibility data: Further evidence for solar forcing on Indian summer monsoon. Geoscience Frontiers 8, 1349-1355

Wen, X., Z. Liu, S. Wang, J. Cheng & J. Zhu, 2016. Correlation and anti-correlation of the East Asian summer and winter monsoons during the last 21,000 years. Nature Communications 7, 11999

Wu, G., Y. Liu, B. He, Q. Bao, A. Duan & F.-F. Jin, 2012. Thermal Controls on the Asian Summer Monsoon. Scientific Reports 2, 404

Xiao, X., S. G. Haberle, J. Shen, X. Yang, Y. Han, E. Zhang & S. Wang, 2014. Latest Pleistocene and Holocene vegetation and climate history inferred from an alpine lacustrine record, northwestern Yunnan Province, southwestern China. Quaternary Science Reviews 86, 35-48

Xu, D., H. Lu, G. Chu, N. Wu, C. Shen, C. Wang & L. Mao, 2014. 500-year climate cycles stacking of recent centennial warming documented in an East Asian pollen record. Scientific Reports 4, 3611

Zhang, E., J. Chang, Y. Cao, W. Sun, J. Shulmeister, H. Tang, P. G. Langdon, X. Yang & J. Shen, 2017a. Holocene high-resolution quantitative summer temperature reconstruction based on subfossil chironomids from the southeast margin of the Qinghai-Tibetan Plateau. Quaternary Science Reviews 165, 1-12

Zhang, E., J. Chang, Y. Cao, H. Tang, P. Langdon, J. Shulmeister, R. Wang, X. Yang & J. Shen, 2017b. A chironomid-based mean July temperature inference model from the south-east margin of the Tibetan Plateau, China. Clim Past 13, 185-199

Zhao, C., Z. Yu, E. Ito & Y. Zhao, 2010. Holocene climate trend, variability, and shift documented by lacustrine stable-isotope record in the northeastern United States. Quaternary Science Reviews 29, 1831-1843

Figure captions

Fig. 1 Map shows the location of Tiancai Lake and surrounding palaeoclimate records that were used for comparison in this study.

Fig. 2. (A) Spectral analysis shows the significant (> 90% and > 95% confidence intervals) periodicities over the last 12 ka in the Tiancai Lake chironomid-based mean

July temperature record. (B) Wavelet power spectrum of the chironomid-based mean July temperature reconstructions after interpolation to evenly spaced data. High power is indicated by red whereas low power is indicated by blue. The areas circled by black solid lines represent the confidence level greater than 95%. The shaded area in the lower part of the diagram indicates the edge effects.

Fig. 3. The Gaussian band-pass filter reveals the signature of the dominant cycles of our Tiancai Lake record (blue dashed lines in A, B and C) and coherence with (A) total solar irradiance (solid pink line) (Steinhilber et al., 2012); (B) Greenland ice core $\delta^{18}O$ record (GISP2) (solid orange line) (Grootes et al., 1993) and (C) Dongge Cave stalagmite $\delta^{18}O$ record (purple solid line) (Wang et al., 2005).

Fig. 4. (A) The Holocene mean July temperature variability at Tiancai Lake shows a comparable pattern with (B) the simulated temperature responses by the overall model in the TraCE-21000 experiment using a state-of-art CGCM: the National Center for Atmospheric Research Community Climate System Model version 3 (NCAR CCSM3) (Liu et al., 2009); (C) the individual simulated temperature response by meltwater influx; (D) ice sheet; (E) CO_2 and (F) orbital forcings alone respectively.

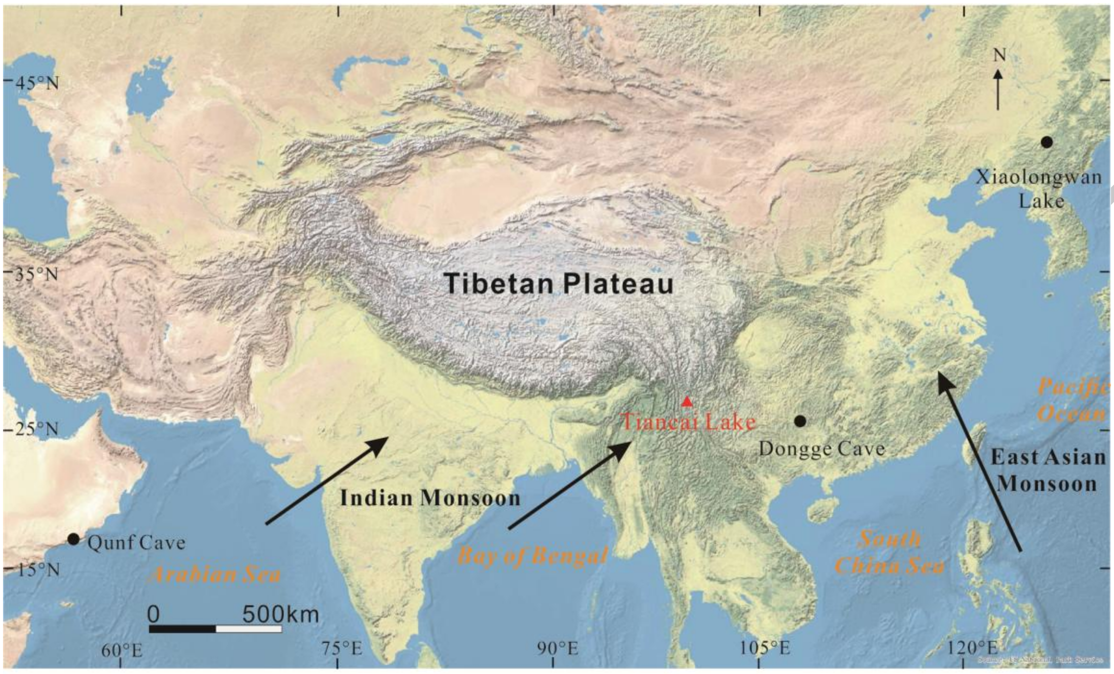

45°N
35°N
25°N
15°N
60°E
75°E
90°E
105°E
120°E
N
Xiaolongwan
Lake
Tibetan Plateau
Tiancai Lake
Dongge Cave
Pacific
Ocean
East Asian
Monsoon
Indian Monsoon
Qunf Cave
Arabian Sea
Bay of Bengal
South
China Sea
0
500km

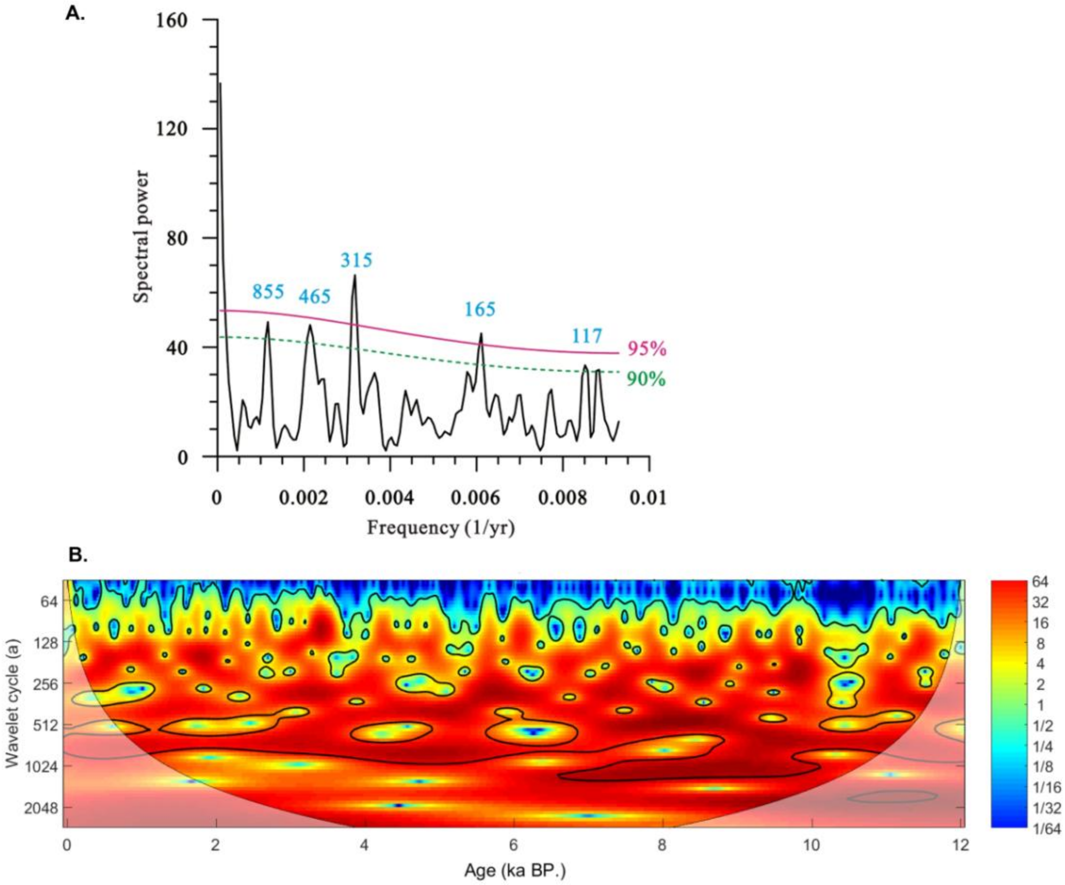
A.
160
120
80
40
0
Spectral power
855
465
315
165
117
95%
90%
0
0.002
0.004
0.006
0.008
0.01
Frequency (1/yr)
B.
64
128
256
512
1024
2048
Wavelet cycle (a)
0
2
4
6
8
10
12
Age (ka BP.)
64
32
16
8
4
2
1
1/2
1/4
1/8
1/16
1/32
1/64

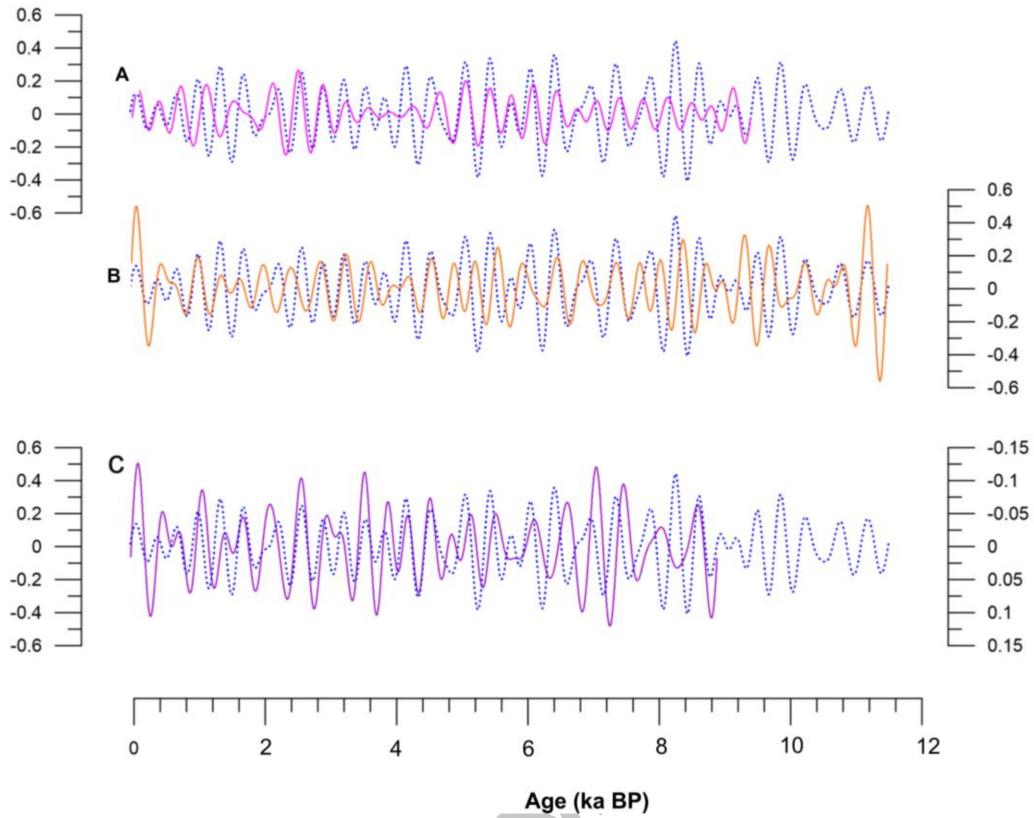
0.6
0.4
0.2
0
-0.2
-0.4
-0.6
A
B
C
0.6
0.4
0.2
0
-0.2
-0.4
-0.6
-0.15
-0.1
-0.05
0
0.05
0.1
0.15
0
2
4
6
8
10
12
Age (ka BP)

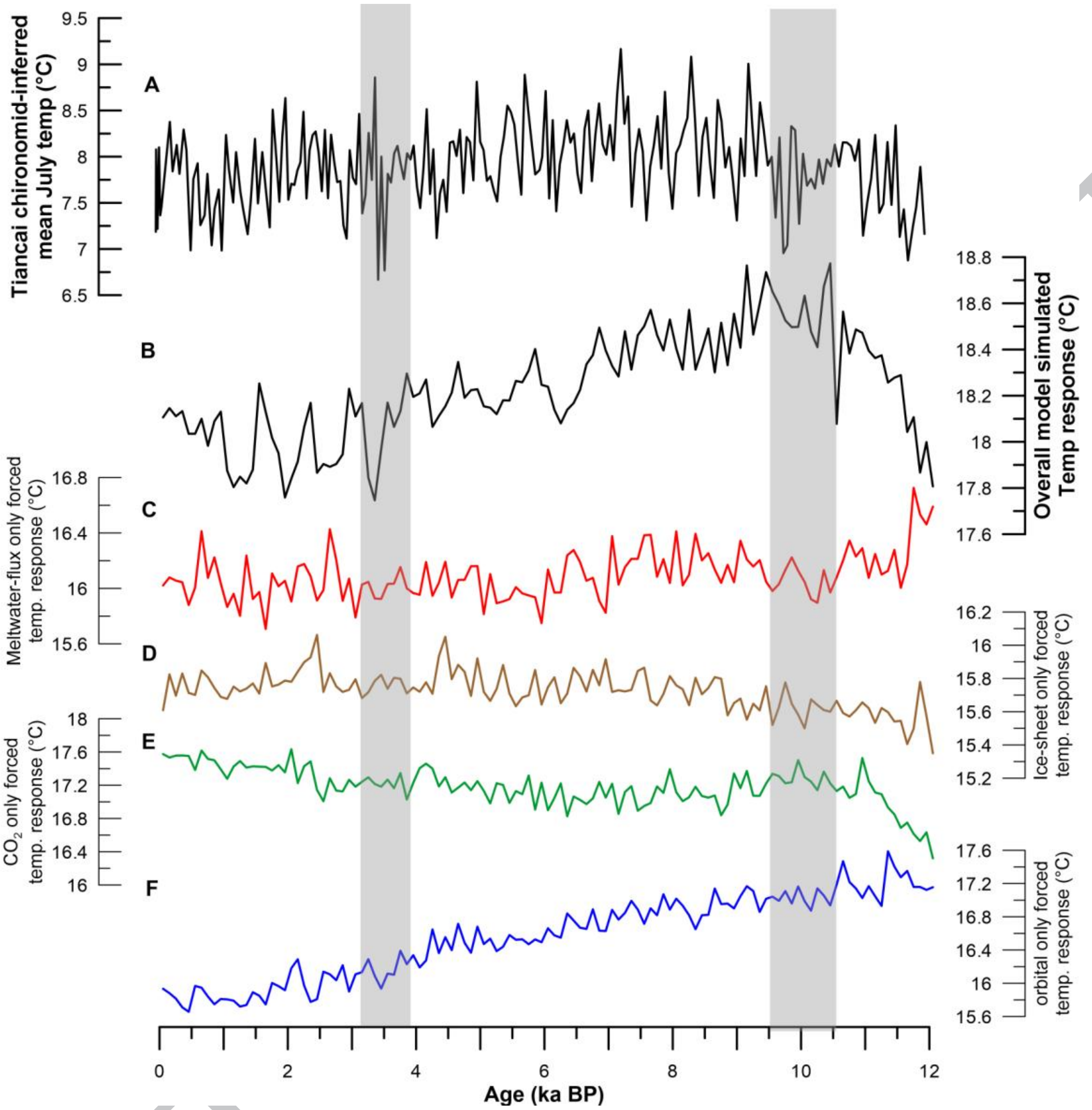

Tiancai chironomid-inferred mean July temp (°C)
9.5
9
8.5
8
7.5
7
6.5
A
B
C
D
E
F
Overall model simulated Temp response (°C)
18.8
18.6
18.4
18.2
18
17.8
17.6
Meltwater-flux only forced temp. response (°C)
16.8
16.4
16
15.6
Ice-sheet only forced temp. response (°C)
16.2
16
15.8
15.6
15.4
15.2
CO2 only forced temp. response (°C)
18
17.6
17.2
16.8
16.4
16
orbital only forced temp. response (°C)
17.6
17.2
16.8
16.4
16
15.6
0
2
4
6
8
10
12
Age (ka BP)

Graphical abstract

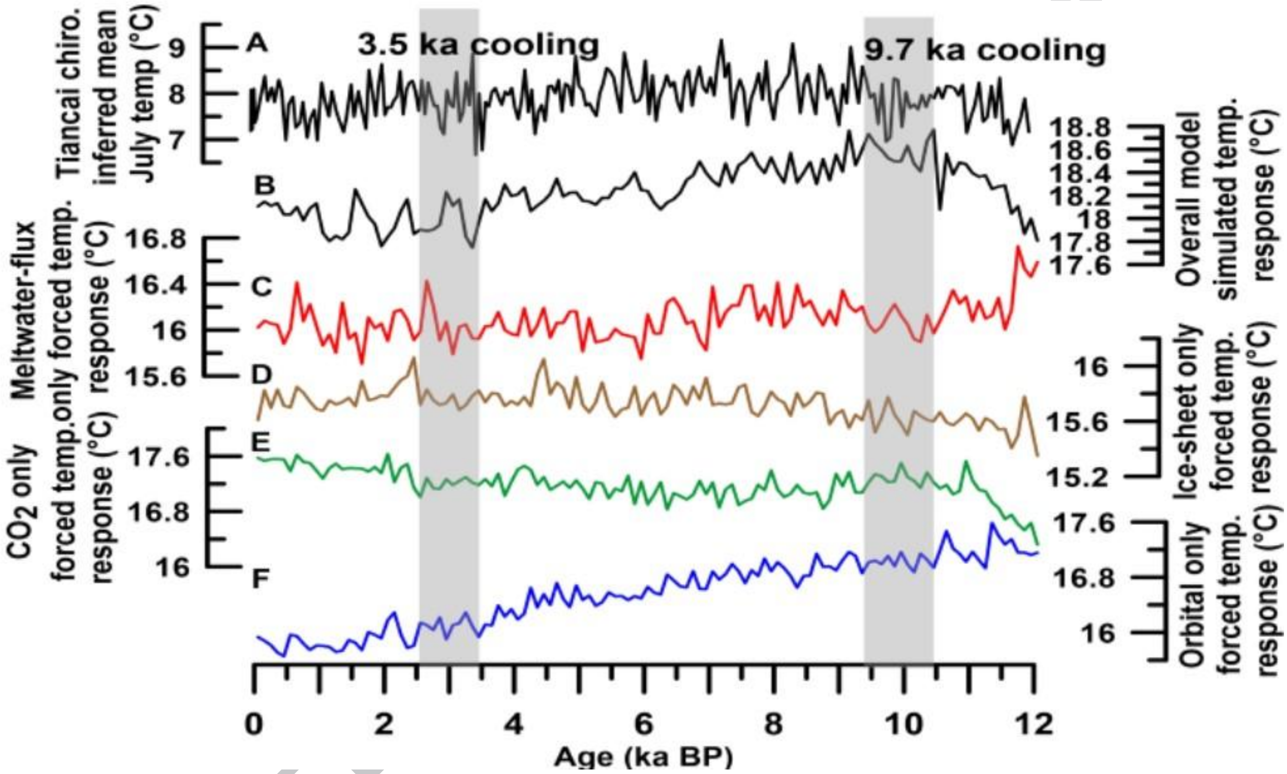

Highlights:

- Solar forcings from lake-based terrestrial summer temperature reconstructions from the Asian monsoon region are explored
- The internal and external forcing mechanisms on the centennial variability of the Asian monsoons and abrupt events are discussed
- High resolution paleoecological record are used to validate paleoclimate modelling outputs